Triple-Shape Polymeric Composites (TSPCs)

By *Xiaofan Luo* and *Patrick T. Mather**

In this paper, the fabrication and characterization of triple-shape polymeric composites (TSPCs) that, unlike traditional shape memory polymers (SMPs), are capable of fixing *two* temporary shapes and recovering sequentially from the first temporary shape (shape 1) to the second temporary shape (shape 2), and eventually to the permanent shape (shape 3) upon heating, are reported. This is technically achieved by incorporating non-woven thermoplastic fibers (average diameter ~760 nm) of a low-T_m semicrystalline polymer into a T_g-based SMP matrix. The resulting composites display two well-separated transitions, one from the glass transition of the matrix and the other from the melting of the fibers, which are subsequently used for the fixing/recovery of two temporary shapes. Three thermomechanical programming processes with different shape fixing protocols are proposed and explored. The intrinsic versatility of this composite approach enables an unprecedented large degree of design flexibility for functional triple-shape polymers and systems.

1. Introduction

Shape memory polymers (SMPs) have been defined traditionally as thermally responsive polymers that can be manipulated to "fix" a temporary shape, and later recovered to their "memorized" permanent shape upon heating.[1–4] A typical shape memory cycle (SMC) involves first deforming the SMP in its rubbery state at an elevated temperature. The deformation is elastic in nature and mainly results in a decrease in conformational entropy of the constituent polymer network chains. Vitrification or crystallization is then triggered by cooling the deformed material, which kinetically traps the SMP in its low-entropy state due to a significant reduction of chain mobility. Macroscopically the material retains its deformed, temporary shape even after releasing the external stress. Shape recovery is later initiated by reheating the material under stress-free or loaded conditions, which allows the relaxation of polymer chain segments (with regained mobility) to their original, entropically favored conformational state.

The field of SMPs has witnessed a rapid growth in the recent years, due to the intrinsic versatility of SMPs in many applications ranging from actuators to sensors and medical devices. A large number of new materials with unprecedented properties have been developed that greatly extend the scope of traditional SMPs. With regard to triggering mechanisms, in addition to direct heating, SMPs have been reported with responsiveness to light,[5] electricity,[6] moisture,[7] solvents[8] and magnetic field.[9] SMPs with unique recovery characteristics have also appeared. For example, two-way shape memory with reversible actuation capabilities was reported for liquid crystalline elastomers (LCEs)[10,11] and semicrystalline networks.[12] "Triple-shape" SMPs – the subject of the present contribution – exhibiting two separate transitions with three different shapes have also been developed.[10,13–19]

Unlike conventional "dual-shape" SMPs which can recover from a temporary shape to a permanent shape, triple-shape SMPs are capable of fixing *two* temporary shapes and recovering sequentially from one temporary shape to the other, and eventually to the permanent shape upon heating. To accomplish this, a triple-shape SMP needs to have two separate shape-fixing mechanisms distinguished by separated thermal transitions in the application temperature range. This naturally leads to a cascade of three elastic modulus plateaus of decreasing magnitude with increasing temperature. Using a molecular approach, Bellin et al.[14,15] synthesized two copolymer networks encompassing 1) poly(ε-caprolactone) (PCL) segments with grafted, short poly(ethylene glycol) (PEG) side chains, and 2) main-chain poly(cyclohexyl methacrylate) (PCHMA) crosslinked with difunctional PCL macromers. Both systems show well separated thermal transitions from 1) PCL melting temperature (T_m) (50–60 °C) and PEG T_m (17 – 39 °C), and 2) PCL (T_m) (50–60 °C) and PCHMA glass transistion temperature (T_g) (~140 °C), each system being able to separately fix two temporary shapes in a programmed thermomechanical cycle. The same group has recently reviewed this work[16] and presented novel actuation of the same compositions.[17] On a similar basis but achieved in a homopolymer (rather than copolymer) system, our group reported a poly(2-*tert*-butyl-1,4,-bis[4-(4-pentenyloxy)benzoyl]hydroquinone) (P5tB) liquid crystalline network (LCN) that is capable of fixing two temporary shapes through first isotropic-nematic transition (~150 °C) and then glass transition (~80 °C).[10] Heating the fixed sample led to complete and sequential recovery of two temporary shapes in a reversed order. Quite recently, Pretsch reported triple shape memory behavior of multiblock polyurethanes,[18] revealing a block copolymer strategy to complement the co-network strategy described above.[14–17] Finally, using a quite different approach at the macroscopic level, Xie et al.[19] reported on triple-shape behavior in

[*] X. Luo, Prof. P. T. Mather
Department of Biomedical and Chemical Engineering
Syracuse Biomaterials Institute
Syracuse NY, 13244 (USA)
E-mail: ptmather@syr.edu

DOI: 10.1002/adfm.201000052

polymer bilayers composed of epoxy thermosets with two different T_gs of 38 and 75 °C. The triple-shape properties were characterized under bending deformations and were shown to be easily tuned by varying the thickness ratio of the two layers. However, the intrinsic asymmetry of this approach may render this system (and thus its shape memory properties) sensitive to the direction of the load. Here we report a new and broadly applicable method for designing and fabricating triple-shape polymeric composites (TSPCs) with well controlled properties.

This approach builds upon our previous experience with the processing of electrochromic nanocomposites by electrospinning[20] and the fabrication of similarly structured shape memory elastomeric composites (SMECs).[21] In the latter system, non-woven PCL microfibers were produced by electrospinning and incorporated into a continuous silicone rubber (Sylgard 184; $T_g \approx -120$ °C) matrix. Overall the material is elastomeric at room temperature while displaying excellent dual-shape memory triggered by the crystallization and melting transitions of the PCL fibers. The large interfacial area intrinsic with this percolating non-woven fiber/matrix morphology greatly facilitated load transfer and load distribution, and led to enhanced shape fixing. In the current study, triple-shape functionality is achieved in a similar system, but with the important difference in selection of the composite matrix, here a T_g-based SMP. This introduces one more transition (in addition to PCL T_m) to the system that can be used to fix a second temporary shape. To further elucidate the general concept, **Scheme 1** illustrates the typical temperature-dependent dynamic mechanical behavior of a TSPC. Deformations (therefore the induced reductions in conformational entropies) within the two rubbery plateaus ($T > T_{m,\,fiber}$ and $T_{g,\,matrix} < T < T_{m,\,fiber}$) can be individually fixed by fiber crystallization and matrix vitrification, respectively. Comparing with previously reported triple-shape SMPs, our approach provides a much larger degree of design flexibility, since one can *separately* tune the two functional components (matrix and fibers) to achieve optimum control of properties. In addition, the final composite is built upon commercially available polymers with a simple fabrication method, which ensures its cost-effectiveness and potential for large-scale manufacturing.

In what follows, we describe the preparation and detailed characterization of the triple-shape polymeric composites, revealing high performance and unique functionality.

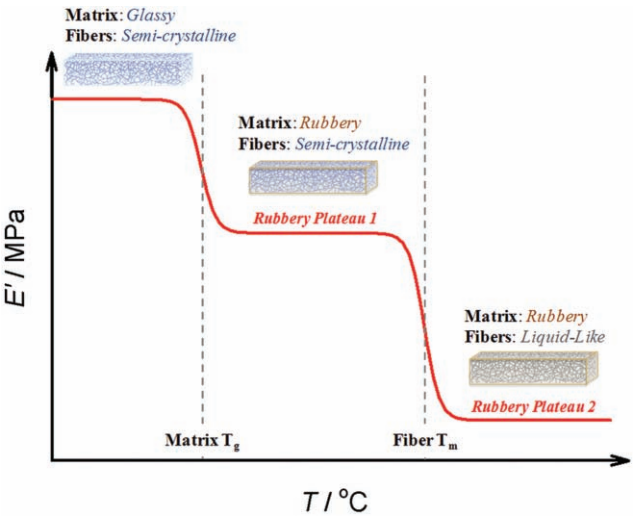

Scheme 1. Schematic illustration of the typical temperature-dependent dynamic mechanical behavior of triple-shape polymeric composites (TSPCs).

2. Results and Discussion

To fabricate TSPCs with the target non-woven fiber/matrix morphology, PCL was first electrospun into non-woven fibers with an average diameter of 760 ± 220 nm (obtained from image analysis; detailed in Supporting Information), shown in **Figure 1A** and B. An epoxy-based copolymer thermoset system reported by Xie and Rousseau[22] was chosen for the SMP matrix. This system is chemically composed of an aromatic diepoxide (diglycidyl ether of bisphenol-A; DGEBA), an aliphatic diepoxide (neopentyl glycol diglycidyl ether; NGDE), and a diamine curing agent (poly(propylene glycol)bis(2-aminopropyl); Jeffamine D230). All chemical structures are shown in **Scheme 2**. Besides the fine control of T_g by copolymerizing DGEBA and NGDE at different ratios, this SMP system features additional advantages of excellent cycle life-time and good thermal/chemical stability. The fabrication of TSPCs was guided by previously established protocols.[21,23] Specifically, a piece of PCL fiber mat was first immersed into the liquid resin mixture, which could easily wet

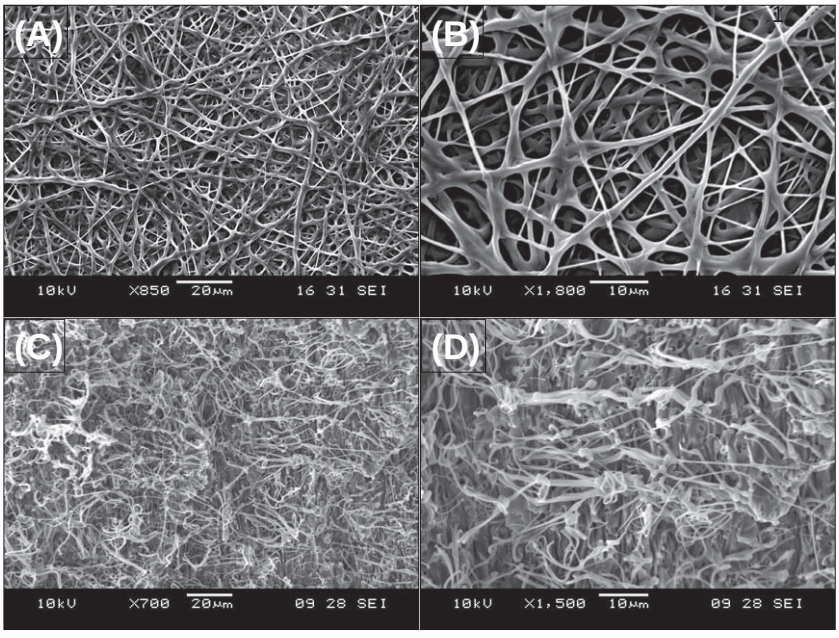

Figure 1. Scanning electron microscope (SEM) images showing A),B) as-spun PCL fibers, and C),D) the cryogenically fractured surface of an Epoxy/PCL TSPC.

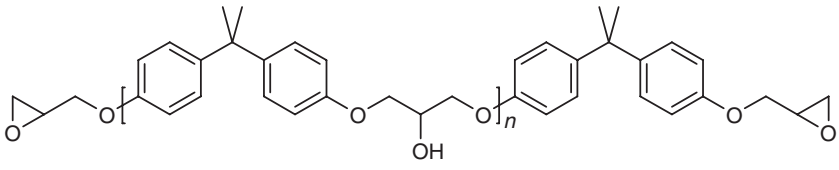

Diglycidyl ether of bisphenol-A (DGEBA)

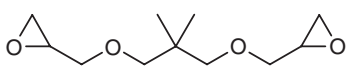

Neopentyl glycol diglycidyl ether (NGDE)

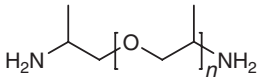

Jeffamine D-230

Scheme 2. The chemical structures of diglycidyl ether of bisphenol-A (DGEBA), neopentyl glycol diglycidyl ether (NGDE), and Jeffamine D-230.

the mat due to its low starting viscosity coupled with favorable interfacial energetics. After carefully removing the excess resin present on the surfaces with a spatula, the system was cured at 40 °C for > 72 h. The bulk structure of fully cured TSPCs was revealed by imaging a cryogenically fractured sample surface (Figure 1C and D), which clearly shows a non-woven, interpenetrating fiber/matrix morphology. The average PCL wt% was measured gravimetrically to be 17.5 ± 0.1%.

The thermal transitions of TSPCs were studied using differential scanning calorimetry (DSC) with the second heating thermograms shown in **Figure 2**. The samples are named according to their compositions, where D and N stand for DGEBA and NGDE, respectively. The number after each letter (D or N) represents the mol% of the component. The curing agent Jeffamine D230 was always incorporated with stoichiometric equivalence (equal number of epoxide rings and amine protons) and is neglected in the sample nomenclature. It can be observed from Figure 2 that all TSPCs show two well-separated thermal transitions, with the step transition at the lower temperature and the peak at the higher temperature attributed to the glass transition of epoxy and the melting of PCL, respectively. The epoxy T_g increased as more DGEBA (the aromatic diepoxide) was used, while PCL T_m remained relatively unchanged and independent of epoxy composition. Furthermore, the epoxy T_gs of TSPCs are almost the same as neat epoxy samples of the same compositions (dashed lines). These findings indicate that there was no or little mixing between epoxy and PCL, and that the two phases (matrix and fibers) behave quite independently. This is advantageous since it allows the control of overall properties of the composite by separately tuning each component.

The temperature-dependent dynamic mechanical behavior is important for SMPs since it is predictive of the shape memory properties and provides information for designing thermomechanical programs for shape fixing and recovery.[2] For this purpose, dynamic mechanical analysis (DMA) was performed for TSPCs under both heating and cooling (**Figure 3**). In good accordance with DSC results, all heating traces (solid lines) showed two separated thermal transitions corresponding to epoxy T_g and PCL T_m, respectively. As a result, two rubbery plateaus, one lying between epoxy T_g and PCL T_m and the other existing above PCL T_m, were observed. The epoxy T_g showed similar dependence on DGEBA content, while PCL melting occurs at almost the same temperature for all three compositions. **Table 1** summarizes the thermal properties of TSPCs determined by both DSC (2nd heating) and DMA (heating). The transition temperatures determined by DMA are noticed to be higher than those determined by DSC, a finding commonly observed for the glass transition and consistent with the observations by Xie and Rousseau on the neat epoxy systems.[22] The overall compositional effect on epoxy T_g can be reasonably described by the Gordon–Taylor equation (see Supporting Information).

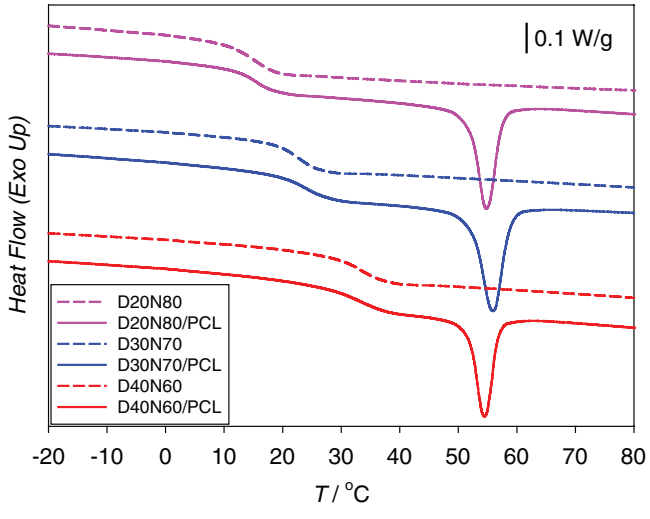

Figure 2. DSC thermograms (2nd heating) of Epoxy/PCL triple-shape composites (solid lines), in comparison with neat epoxies of the same compositions (dashed lines). The heating rate was 10 °C for all the samples.

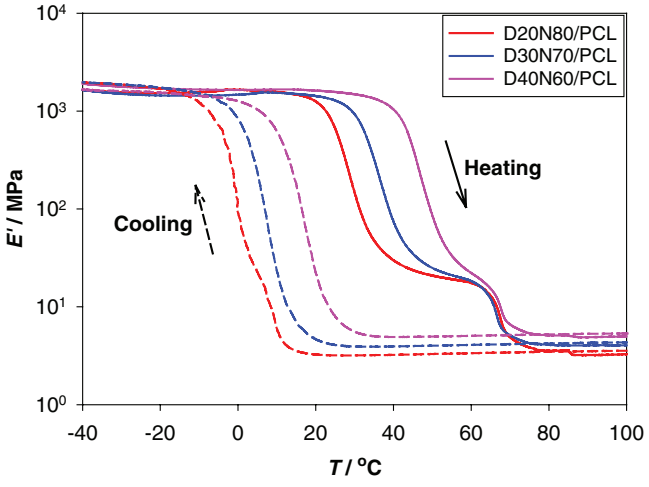

Figure 3. DMA results for Epoxy/PCL TSPCs under both heating (solid lines) and cooling (dashed lines). The heating and cooling rates were both 3 °C min^{-1}.

Table 1. Thermal properties of TSPCs measured by DSC and DMA.

Sample	Epoxy T_g from DSC [°C]	PCL T_m from DSC [°C]	PCL ΔH_m [J g^{-1}]	Epoxy T_g from DMA [°C]	PCL T_m from DMA [°C]
D20N80/PCL	15.3	54.8	9.7	23.0	65.2
D30N70/PCL	24.0	56.0	10.4	30.5	64.4
D40N60/PCL	33.2	54.5	9.7	41.4	66.2

Another noticeable feature in the DMA results is the fact that the second rubbery moduli (T > PCL T_m) decreased with increasing NGDE content. The same trend was also observed for neat epoxies (see Supporting Information). This is somewhat unexpected since more NGDE would lead to higher crosslinking density (since its molecular weight is smaller than DGEBA) therefore higher rubbery modulus. However this can be rationalized in terms of chain flexibility. Considering the equation of rubber elasticity with an additional front factor ϕ,[24]

$$G_R = \varphi \frac{\rho RT}{M_c} \quad (1)$$

where G_R is the elastic shear modulus, ρ is the density, T is the temperature, and M_c is the average molecular weight between crosslinks (note: $E_R = 3G_R$ for isotropic elastomers). Here, ϕ is defined by Urbaczewski–Espuche et al.[24] as the ratio of the mean squared end-to-end distance of a network chain to that of a randomly coiled (Gaussian) chain. Due to the relatively low molecular weights of NGDE (216.3 g mol^{-1}) and DGEBA (340.4 g mol^{-1}), it is reasonable to postulate (and apparent from our results) that the conformation of such segments in the network is non-Gaussian ($\phi \neq 1$). In principal, the incorporation of NGDE should reduce M_c; however, it is compensated by a larger degree of reduction in ϕ, which we interpret to be due to the higher chain flexibility compared to DGEBA (aliphatic vs. aromatic). The overall effect is a decrease in rubbery modulus.

The cooling DMA results (dashed lines in Figure 3) reveal quite different features from the heating traces. Except D20N80/PCL in which the two step transitions can still be identified, in D30N70/PCL and D40N60/PCL the two transitions (epoxy vitrification and PCL crystallization) are largely merged together into a single step. This is primarily due to the difference in kinetics between the two transitions (crystallization being slower) under the same cooling rate (3 °C min^{-1}). This imposes some challenges to shape fixing since two separated transitions are needed to fix two different temporary shapes. Therefore specifically designed thermomechanical programs, rather than simple deformation-cooling steps, are needed for TSPCs. In what follows, we will explore three different fixing methods and analyze the resulting SMCs. It should be noted that, although D30N70/PCL was chosen to demonstrate the triple-shape behavior, the principles involved in all fixing methods are equally applicable to other compositions.

The first fixing method involved an isothermal annealing step at an intermediate temperature to induce PCL crystallization while maintaining the epoxy matrix in the rubbery state. Isothermal DMA was first performed to isolate an annealing temperature useful for strain fixing. For this experiment, the sample (a rectangular film under oscillatory tension) was first equilibrated at 80 °C, cooled to an intermediate temperature at 3 °C min^{-1}, and held isothermally for 60 min. Four isothermal temperatures of 50, 40, 30, and 20 °C were investigated with the corresponding time-dependent storage modulus (E') profiles shown in **Figure 4** for both D30N70/PCL and D30N70 (neat epoxy). It is observed that 50 °C was too high for both transitions, given the flatness of E' over time. However, at 40 °C, the storage modulus of D30N70/PCL showed an increase that significantly exceeded D30N70. This is clearly due to the isothermal crystallization of PCL, since the presence of PCL is the only structural difference between the two materials. When the temperature was further decreased to 30 and 20 °C, both transitions took place in a time-overlapping fashion and the two samples showed similar storage modulus time evolutions. Overall, it can be concluded that 40 °C is the best temperature (among those studied) for first-stage shape fixing by PCL crystallization without epoxy matrix vitrification.

The triple-shape memory behavior of the D30N70/PCL utilizing a 40 °C annealing step was characterized quantitatively and the results described below (**Figure 5A**). A uniaxially loaded dumbbell specimen (ASTM D638, see Experimental section for details) of D30N70/PCL was first deformed at 80 °C (above both epoxy T_g and PCL T_m) by ramping the force at 0.05 N min^{-1} until a strain of 15% was achieved. The sample was then cooled to 40 °C at 3 °C min^{-1} while holding the external force constant, followed by an isothermal hold for 60 min. The external load was released by unloading the force back to 0.001 N (a small preload). This finished the fixing of the first temporary shape

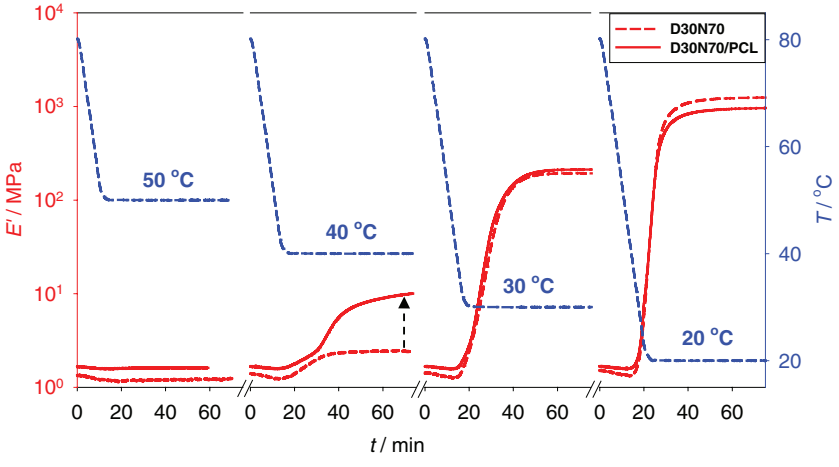

Figure 4. Isothermal DMA results for D30N70/PCL in comparison with D30N70 at different temperatures of 50, 40, 30, and 20 °C. In each case, the sample was first equilibrated at 80 °C, cooled to the target isothermal temperature at 3 °C min^{-1} and held isothermally for 60 min. The dashed arrow indicates the contribution from PCL crystallization (details are discussed in the main text).

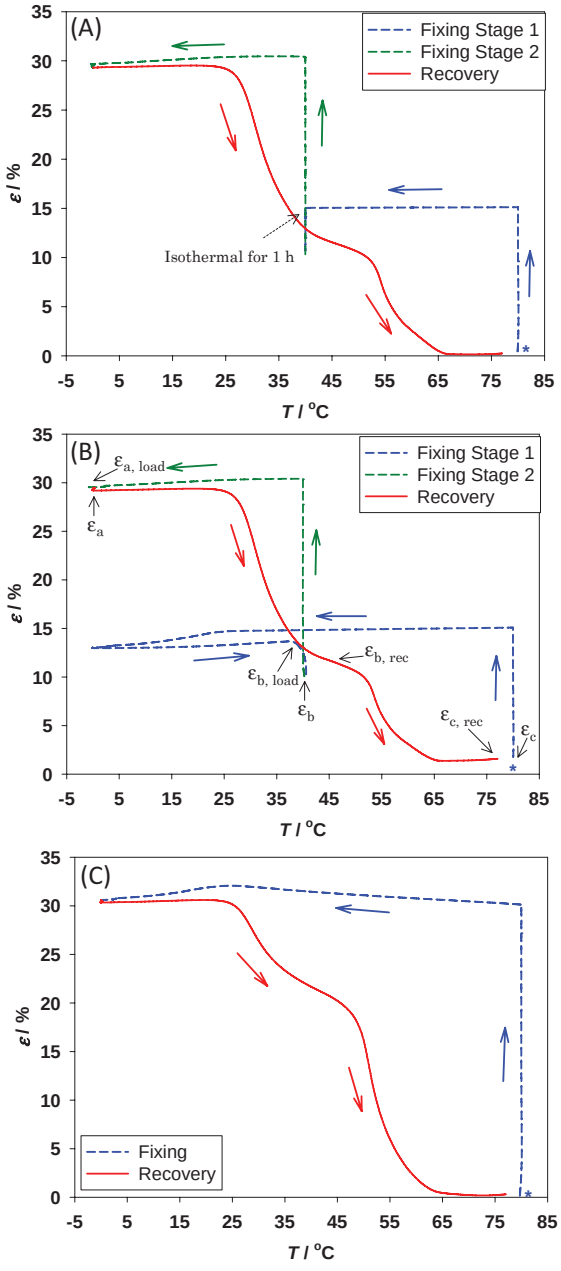

Figure 5. Triple-shape SMCs corresponding to different fixing protocols. The blue star in each graph indicates the onset of SMC. Details are discussed in the main text.

and is represented as the blue dashed line (Fixing Stage 1) in Figure 5A. The shape memory testing continued by reloading the sample at 40 °C using the same force rate of 0.05 N min^{-1} until a strain of 30% was achieved. The temperature was further reduced to 0 °C followed by the second release of external force. This led to fixing of the second temporary shape and is shown as the green dashed line (Fixing Stage 2) in Figure 5A. Sequential recovery of the two fixed deformations – in reverse order – was finally triggered by heating the sample to 80 °C at 3 °C min^{-1} (red solid line in Figure 5A). For the sake of clarity, here we arbitrarily designate the first temporary shape fixed at 40 °C, the second temporary shape fixed at 0 °C and the permanent shape to be shapes **b**, **a**, and **c**, respectively.

It can be seen from the results of Figure 5A that, while the first unloading at 40 °C led to some instantaneous strain recovery (incomplete fixing of shape **b**), the fixing of shape **a** at 0 °C was almost perfect. The heating curve clearly showed two sequential recovery transitions, first from shape **a** to **b** and then from **b** to **c**. The two transition temperatures correlate well with the epoxy T_g and PCL T_m, respectively.

Although the first fixing method resulted in good triple-shape performance, in particular good fixing and recovery of the two temporary shapes, the lengthy isothermal step involved in the thermomechanical programming is not desirable and may render some practical applications difficult. To overcome this, we designed a second fixing method that does not require any isothermal holding step and therefore can dramatically increase the rate of shape fixing for shape **b**. Similar to the first fixing method, the current method involved first loading the sample to 15% strain at 80 °C under the same force rate (0.05 N min^{-1}). The temperature was then reduced continuously to 0 °C (instead of to 40 °C as in the first method), during which time both the epoxy vitrification and *rapid* PCL crystallization took place. Due to their existence as separate phases, these two processes do not interfere with each other. Following this step, the sample was reheated to 40 °C with the epoxy passing through its glass transition to a rubbery state, while the PCL phase remained semicrystalline since the temperature was still below its T_m (see the heating DMA trace for D30N70/PCL in Figure 3). The material was at essentially the same state as the isothermally annealed material, but achieved with a much shorter time than in the previous method (ca. 33 min shorter with the current heating/cooling rate of 3 °C min^{-1}). It should be noted that, in reality this time reduction can be more significant since the second method can be shortened by enhanced heat transfer (the selection of 3 °C min^{-1} in the shape memory experiments was instrument-limited) while the first method requires at least 60 min due to slow crystallization kinetics (Figure 4). The external load was then released at 40 °C to finish the fixing of shape **b**, and the entire fixing step is plotted as the blue dashed line in Figure 5B. The subsequent fixing of shape **a** as well as the recovery were conducted similarly to the first method. Briefly, the sample was reloaded to 30% strain at 40 °C, cooled to 0 °C, unloaded and finally heated to 80 °C for sequential recovery: **a** → **b** → **c**. The recovery profile (red solid line in Figure 5B) in the current method is indeed quite similar to the one in the first method.

We further explored whether triple-shape behavior can be achieved in a process involving only a single fixing step. The corresponding SMC experiment was carried out as follows and with results shown in Figure 5C. The sample was first stretched to 30% strain at 80 °C, cooled to 0 °C while holding the external force, and unloaded to finish shape fixing (in this case, the fixing of shape **a**). During heating (3 °C min^{-1} to 80 °C), the strain recovered in two separated steps (red solid line in Figure 5C), indicating a seemingly triple-shape behavior. Similar observations were reported recently by Behl et al.[13] for their PCHMA-PCL copolymer networks. The origin of this phenomenon lies in the fact that the PCL fibers alone are not sufficient in fixing the total strain, explained further below, but are capable

of resisting complete recovery of the epoxy matrix while they are in the semicrystalline state. When the deformed sample is cooled from 80 to 0 °C, the strain (30%) is fixed by both PCL crystallization and epoxy vitrification. When the temperature is raised to $T_{g,\ epoxy} < T < T_{m,\ PCL}$, the devitrified epoxy network attempts to elastically recover to its equilibrium state. However, in the same temperature range PCL still exists as rigid, semicrystalline fibers and is resisting this matrix recovery. As a consequence, the overall composite only recovers to the point at which the two competing factors balance each other (matrix recovery force = fiber network resistive force). This accounts for the first step-recovery seen in Figure 5C. The remaining strain could only recover upon further heating to $T > T_{m,\ PCL}$.

The observed two-step recovery behavior is due to the fact that the PCL fibers can only partially resist the matrix recovery. If, on the other hand, PCL fiber network could resist all (>99%) the matrix recovery, i.e., fix all the temporary shape on its own, the first recovery at epoxy T_g would not have been seen. This can potentially be achieved through enhancing the mechanical stiffness of the constituent fibers (therefore generating a larger resistive force) by densifying the mat (increasing its wt% in the composite)[23] or introducing more inter-fiber bonding.[25] Understanding this, we contend that the two-step recovery witnessed under this one-step fixing method is not strictly a "triple-shape" phenomenon, since the first temporary shape (shape **b**) is not separately defined in the thermomechanical cycle and the relative proportions of the two recovery transitions depend only on the relative mechanical contributions from the two (matrix and fibers) components. It is merely a two-step recovery of a single temporary shape. Nevertheless, as also noted by Behl et al.,[13] this finding is still of merit and may find practical relevance to applications in which stepped recoveries are desired.

The triple-shape properties of TSPCs were further quantified by calculating the fixing ratios (R_f) and recovery ratios (R_r) for all the SMCs investigated. The two characteristic ratios are defined specifically as

$$R_f(x) = \frac{\varepsilon_x}{\varepsilon_{x,\mathrm{load}}} \times 100\% \quad (2)$$

$$R_r(x \rightarrow y) = \frac{\varepsilon_x - \varepsilon_{y,\mathrm{rec}}}{\varepsilon_x - \varepsilon_y} \times 100\% \quad (3)$$

Here $\varepsilon_{x,\mathrm{load}}$, ε_x, and $\varepsilon_{x,\mathrm{rec}}$ stand for the strain before unloading, the strain after unloading, and the strain after recovery for shape x (x can be **a**, **b** or **c**, the same for y). For shape **c**, ε_c is simply the starting strain (primarily thermal strain). $\varepsilon_{b,\mathrm{rec}}$ is determined from the midpoint of the intermediate plateau in the recovery curve. All of the strains involved in these calculations are labeled for the second fixing method (Figure 5B) for clarity. For each SMC, two R_f values corresponding to the fixing of temporary shapes **a** and **b**, and three R_r values for the recoveries from **a** to **b**, **b** to **c**, and **a** to **c**, can be calculated. The results are summarized in **Table 2** for the three TSPCs investigated. It should be noted that, for D20N80/PCL, all the shape fixing methods were identical to D30N70/PCL discussed above. For D40N60/PCL, the deformation temperature for shape **a** in the first and second fixing methods was raised from 40 °C (as in the cases of D20N80/PCL and D30N70/PCL) to 50 °C to accommodate its higher T_g (41.4 °C as determined from DMA). The raw SMC graphs (similar to Figure 5) as well as additional experimental details for D20N80/PCL and D40N60/PCL are available in Supporting Information. It can be seen from Table 2 that, similar among all TSPCs, the fixing of shape **a** and all the shape recoveries are nearly perfect (R_f(a) and R_r values close to 100%). The incomplete fixing of shape **b**, as discussed above, is due to the insufficiency of the PCL fiber network to resist all the matrix recovery at $T_{g,epoxy} < T < T_{m,\ PCL}$, and can be improved via enhancing the mechanical stiffness of PCL fibers by various means, as suggested above.

Table 2. Fixing and recovery ratios calculated for TSPCs tested using three different fixing methods. All the numbers represent percentages (%).

Sample	Fixing Method	R_f(a)	R_f(b)	R_r(a → b)	R_r(b → c)	R_r(a → c)
D20N80/PCL	Method 1	98.7	74.4	89.8	91.5	97.3
	Method 2	98.7	76.7	90.1	92.9	97.8
	Method 3	99.4	–	–	–	96.2
D30N70/PCL	Method 1	99.0	73.9	93.4	102.1	100.7
	Method 2	97.0	73.5	91.6	101.8	100.6
	Method 3	99.3	–	–	–	99.5
D40N60/PCL	Method 1	99.2	64.1	88.8	99.5	99.8
	Method 2	99.2	59.8	89.3	98.3	99.5
	Method 3	99.5	–	–	–	99.7

Finally, we present a visual demonstration showing the triple-shape behavior of a representative TSPC. A fully cured D30N70/PCL sample was cut into a rectangular film of dimensions 30 mm × 6.8 mm × 0.6 mm (shape **c**). A protocol similar to the second fixing method discussed above was utilized for shape fixing, as we now describe. The sample was first immersed in a water bath at 80 °C, quickly deformed to an "M" shape and quenched in a second bath with ice/water mixture at 0 °C. After immersing into a third water bath at 40 °C, the sample showed some minor recovery due to the incomplete fixing of PCL, but a major part of deformation was retained (since R_f(b) is still greater than 70%) and a temporary shape **b** similar to **Figure 6B** was fixed. Maintaining the sample temperature at 40 °C, the sample was further manipulated by winding around a glass rod and immersed into the ice/water bath again. This led to fixing of the second temporary shape **a** as shown in Figure 6A. After immersing the sample with shape **a** back into the water bath at 40 °C, it quickly recovered to shape **b** as shown in Figure 6B, which further recovered to its permanent shape **c** after immersing into the water bath at 80 °C as shown in Figure 6C. A time-continuous movie showing the sequential recovery process is available in Supporting Information.

3. Conclusions

To briefly conclude, a series of triple-shape polymeric composites (TSPCs) have been developed using a unique while broadly applicable fiber/matrix composite approach. Besides the demonstrated high performance in the form of triple-shape

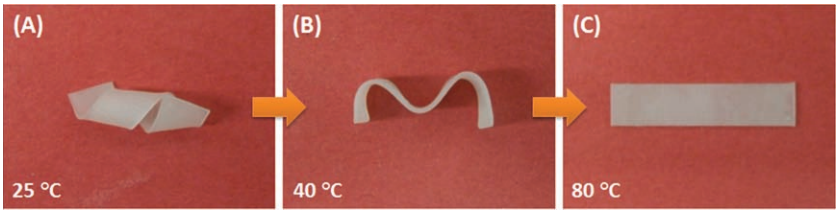

Figure 6. Photographs showing the sequential recovery of D30N70/PCL from temporary shape **a** (A), to temporary shape **b** (B), and to permanent shape **c** (C). The experimental details on shape fixing and recovery can be found in the main text.

properties for our TSPCs, it is significant that our composite approach affords a large degree of design flexibility that may enable the design of triple-shape systems for target applications. For example, one can control the transition temperatures by simply selecting different polymers for the fibers and the matrix, or separately functionalize them (either chemically or physically) to achieve other novel functions (in addition to triple-shape) such as controlled drug delivery or reversible adhesion. Future work may focus on 1) achievement a more in-depth understanding of the structure-property relationships in TSPCs, with the ultimate goal being to mathematically model their behavior, and 2) development of multifunctional triple-shape systems using this general approach.

4. Experimental Section

Materials: All chemicals used, including DGEBA, NGDE, Jeffamine D230, and PCL (nominal M_w = 65 000 g mol^{-1}) were purchased from Sigma-Aldrich and used as received.

Electrospinning of PCL: The solution for electrospinning was prepared by dissolving PCL pellets (2 g) in a mixed chloroform/DMF solvent ($V_{chloroform}$:V_{DMF} = 8:2, V_{total} = 10 mL). Electrospinning was conducted using a custom-built setup that consists of a high voltage power supply (Agilent E3630A), a syringe pump (KDS100, KD Scientific) and a rotating drum collector. A constant flow rate of 1 mL h^{-1}, along with an applied voltage of 15 kV and a tip-to-collector distance of 10 cm was used. The collecting drum (diameter = 5 cm) was rotated at a constant velocity of 400 rpm with a slow, oscillatory horizontal translation with an amplitude of 6 cm that yields uniform mat thicknesses.

Fabrication of TSPCs: The Epoxy/PCL TSPCs were fabricated following a method similar to previous reports[21,23] for other electrospun composites. DGEBA was first preheated at 70 °C to melt all the crystals that may be present. NGDE and Jeffamine D-230 of calculated amounts were added and quickly mixed by vigorous manual stirring with a glass rod (~1 min) until a clear, colorless and low-viscosity mixture was obtained. A piece of electrospun PCL fiber mat with known mass was submerged in the resin mixture and maintained there for 20–30 min. After carefully removing the extra resin on the surfaces, the resin-loaded composite was cured at 40 °C for > 72 h.

Morphological Characterization: Scanning electron microscopy (SEM) was used to study the morphologies of electrospun PCL fiber mat and Epoxy/PCL TSPCs. For the latter, a fully cured composite was cryogenically fractured in liquid nitrogen to preserve the bulk morphology. Both the top surface of an as-spun PCL mat and the fractured surface of the TSPC were sputter coated with gold and examined by a JEOL JSM5600 SEM instrument. A typical accelerating voltage of 10 kV was used.

Thermal Characterization: The thermal properties of Epoxy/PCL composites as well as neat epoxy samples were characterized using DSC. Samples (typical mass ~3–5 mg) were encapsulated in Tzero aluminum pans and examined on a Q200 (TA Instruments) DSC instrument. For each experiment, the sample was first heated from –40 °C to 120 °C, cooled back to –40 °C, and finally heated to 120 °C. All heating/cooling rates were 10 °C min^{-1}. The epoxy T_g and PCL T_m were determined from the midpoint of the step transition and the melting peak temperature, respectively. The melting enthalpy (ΔH_m) was calculated by integrating the melting peak.

DMA: The thermomechanical properties of Epoxy/PCL composites were characterized using a Q800 DMA (TA Instruments). In each case, a rectangular film (typical dimensions = 5 mm × 2 mm × 0.6 mm) was loaded under tension and an oscillatory deformation with an amplitude of 10 μm, a frequency of 1 Hz and a "force track" (ratio of static to dynamic force) of 108% was applied. The temperature was first equilibrated at –90 °C, ramped to 150 °C at a linear rate of 3 °C min^{-1}, kept isothermal for 5 min and finally ramped back to –90 °C at the same rate. The epoxy T_g and PCL T_m were determined from the onset points of storage modulus (E') transitions.

Shape Memory Characterization: Quantitative characterization of triple-shape properties was conducted using the same Q800 DMA instrument under controlled force mode. Since the experiments involved large-strain tensile deformations, a dumbbell geometry guided by ASTM D638 was adopted (detailed dimensions are provided in Supporting Information). The sample thickness varied between 0.6 to 0.7 mm. Prescribed thermomechanical programs corresponding to different fixing protocols were conducted, the details of which are discussed in Results and Discussion section.

Supporting Information

Supporting Information is available online from Wiley InterScience or from the author.

Acknowledgements

The authors acknowledge Prof. Jeremy Gilbert (Syracuse University) for the access to the SEM instrument. Partial support from AFOSR (FA9550-09-1-0195) and NSF (DMR-0758631) is gratefully acknowledged.

Received: January 10, 2010
Revised: May 3, 2010
Published online: July 1, 2010

[1] A. Lendlein, S. Kelch, *Angew. Chem. Int. Ed.* **2002**, *41*, 2034.
[2] C. Liu, H. Qin, P. T. Mather, *J. Mater. Chem.* **2007**, *17*, 1543.
[3] P. T. Mather, X. F. Luo, I. A. Rousseau, *Annu. Rev. Mater. Res.* **2009**, *39*, 445.
[4] I. A. Rousseau, *Polym. Eng. Sci.* **2008**, *48*, 2075.
[5] A. Lendlein, H. Y. Jiang, O. Junger, R. Langer, *Nature* **2005**, *434*, 879.
[6] Y. J. Liu, H. B. Lv, X. Lan, J. S. Leng, S. Y. Du, *Compos. Sci. Technol.* **2009**, *69*, 2064.
[7] B. Yang, W. M. Huang, C. Li, L. Li, *Polymer* **2006**, *47*, 1348.
[8] H. B. Lv, J. S. Leng, Y. J. Liu, S. Y. Du, *Adv. Eng. Mater.* **2008**, *10*, 592.
[9] R. Mohr, K. Kratz, T. Weigel, M. Lucka-Gabor, M. Moneke, A. Lendlein, *Proc. Natl. Acad. Sci. USA* **2006**, *103*, 3540.
[10] H. H. Qin, P. T. Mather, *Macromolecules* **2009**, *42*, 273.

[11] I. Kundler, H. Finkelmann, *Macromol. Rapid Commun.* **1995**, *16*, 679.
[12] T. Chung, A. Rorno-Uribe, P. T. Mather, *Macromolecules* **2008**, *41*, 184.
[13] M. Behl, I. Bellin, S. Kelch, W. Wagermaier, A. Lendlein, *Adv. Funct. Mater.* **2009**, *19*, 102.
[14] I. Bellin, S. Kelch, R. Langer, A. Lendlein, *Proc. Natl. Acad. Sci. USA* **2006**, *103*, 18043.
[15] I. Bellin, S. Kelch, A. Lendlein, *J. Mater. Chem.* **2007**, *17*, 2885.
[16] M. Behl, A. Lendlein, *J. Mater. Chem.* **2010**, *20*, 3335.
[17] U. N. Kumar, K. Kratz, W. Wagermaier, M. Behl, A. Lendlein, *J. Mater. Chem.* **2010**, *20*, 3404
[18] T. Pretsch, *Smart Mater. Struct.* **2010**, *19*, 015006
[19] T. Xie, X. C. Xiao, Y. T. Cheng, *Macromol. Rapid Commun.* **2009**, *30*, 1823.
[20] S. Y. Jang, V. Seshadri, M. S. Khil, A. Kumar, M. Marquez, P. T. Mather, G. A. Sotzing, *Adv. Mater.* **2005**, *17*, 2177.
[21] X. F. Luo, P. T. Mather, *Macromolecules* **2009**, *42*, 7251.
[22] T. Xie, I. A. Rousseau, *Polymer* **2009**, *50*, 1852.
[23] J. Choi, K. M. Lee, R. Wycisk, P. N. Pintauro, P. T. Mather, *Macromolecules* **2008**, *41*, 4569.
[24] E. Urbaczewski-Espuche, J. Galy, J. F. Gerard, J. P. Pascault, H. Sautereau, *Polym. Eng. Sci.* **1991**, *31*, 1572
[25] S. J. Lee, S. H. Oh, J. Liu, S. Soker, A. Atala, J. J. Yoo, *Biomaterials* **2008**, *29*, 1422.